The HOMFLY-PT polynomial of the Conway and Kinoshita-Terasaka Knots

Kenneth C. Millett
Department of Mathematics
University of California, Santa Barbara, CA, USA
Eleni Panagiotou
University of Tennessee at Chattanooga
Chattanooga, TN, USA

November 15, 2021

Abstract

We study the 11 edge equilateral polygonal representations of the Conway and Kinoshita-Terasaka knots. By removing edges of the configurations, we study the HOMFLY-PT spectrum of the open arc conformations using DMS closures whose superposition defines an average HOMFLY-PT polynomial of the open arc. Defining the spread of this polynomial gives a measure of the complexity of the knotting entanglement of the open arc. The spectrum, its superposition polynomial and the associated spread provide new methods to compare the Conway and Kinoshita-Terasaka knots and provide new information supporting the view that despite their similarities, the Conway knot is more entangled and more complex than the Kinoshita-Tereasaka knot.

1 Introduction

In this paper, we introduce a new application of the HOMFLY-PT polynomial for a polygonal representation of a knot that provides a tool with which to detect differences betweek the Conway and Kinoshita-Terasaka knots. More precisely, we will explore the HOMFLY-PT polynomial, [4], of some examples of open 10 edges equilateral polygonal arc presentations of the classical Conway [2] and Kinoshita-Terasaka [9] knots. To do so, we estimate the superposition of the spectrum of HOMFLP-PY polynomials taken over the closures of the open chains employing a uniform sampling of points on extremely large 2-spheres centered at the center of mass of the open chains. This method was created to study the knotting of open arcs modeling proteins, with the objective of identifying the dominant knot type (the best approximation of an open curve by a classical knot) [13, 15]. The superpositon of the knot spectrum does not

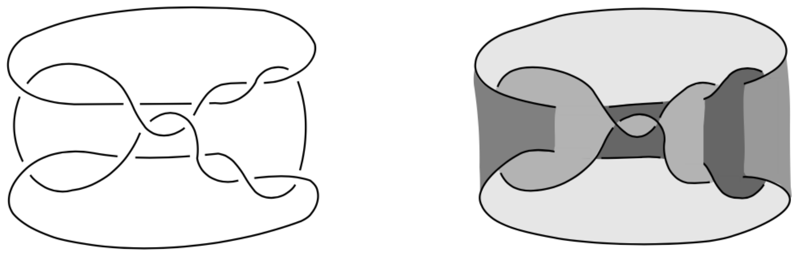

Figure 1: With a slight re-organization of a traditonal presentation one has a ribbon presentation of the Kinoshita-Terasaka knot showing that it is smoothly slice, Hom [6]

approximate an open curve by a knot type but, instead, aims at revealing the complexity of the open arc. By applying the average HOMFLY-PT polynomial to subchains of the Conway and Kinoshita-Terasaka knots we display underlying features that make their differences visible even though their HOMFLY-PT polynomials are the same.

The Conway knot is an 11 crossing non-alternationg knot of genus 3, the mirror of K11n34 in the Thistlethwaite notation. The Kinoshita-Terasaka knot is an 11 crossing non-alternationg knot of genus 2, the mirror of K11n42 in the Thistlethwaite notation, figure 2, and a mutant of the Conway knot [10]. They were first shown to be distinct by Riley [20] who proved that the fundamental groups of their complements in the 3-sphere are different and, later, Gabai [5] proved they were of genus 3 and 2, respectively. More recently, Morton and Cromwell [16] employed polynomials of satellites to distinguish some mutants, including the Conway and Kinoshita-Terasaka knots. While the Kinoshita-Terasaka knot was known to be smoothly slice, figure 1, in 2020 Lisa Piccirillo proved that the Conway knot is not smoothly slice thereby resolving a 50 year knot theory problem [18].

Our study is based on 11 edge equilateral polygonal models of the two knots provided to us by Eddy and Shonkwiler [3]. We have carefully perturbed the polgyons so to expand them by increasing the minimum distance between non-adjacent edges in each polygon, Figure 3. Open arc examples are then created by removing an edge of the polygonal model, or a subsegment of an edge, thereby creating open polygons that "display" the respective knot types.

For a selected oriented open polygonal chain, the estimation of the superposition of the spectrum of HOMFLY-PT polynomials is achieved by determining the associated HOMFLY-PT polynomial of terminal closures in directions selected from a uniformly distributed collection of 6400 directions on the directional 2-sphere, [13]. This provides an approximation of the probability distribution of HOMFLY-PT polynomials of the closures and, thus, an estimation of the superposition by integration of the HOMFLY-PT pdf over the S^2

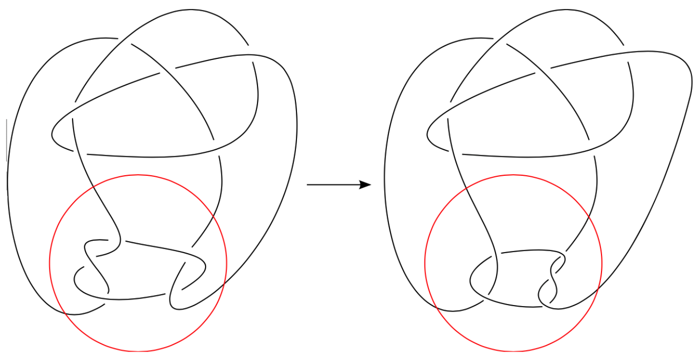

Figure 2: The Kinoshita-Terasaka knot, on the left, and the Conway knot, on the right, are related by the indicated mutation (Wikipedia) and therefore their HOMFLY-PT polynomials are equal: $(2*\ell^{-2}+7+6*\ell^{2}+2*\ell^{4})+(-3*\ell^{-2}-11-11*\ell^{2}-3*\ell^{4})*m^{2}+(\ell^{-2}+6+6*\ell^{2}+\ell^{4})*m^{4}+(-1-\ell^{2})*m^{6}$.

space of directions. One of the fundamental properties of the DMS method is that the proportion of knot types converges to that of the closed chain as the distance between the termini of the chain goes to zero. This, however, depends on the location of the gap in the chain and its size. We will explore this dependence for both knots. In addition, as was observed in the study of protein structures, the HOMFLY-PT spectrum depends on the specific geometry of the chain [15, 19, 22]. We will numerically exploit the influence of the location of the gap in a closed chain as well as the effect of the spatial geometry of the chain. In order to detect differences between the Conway knot and the Kinoshita-Terasaka knot, we will gather the spectra associated to the collection of edge gaps of the knot presentations and calculate the associated superpositions. As the superposition HOMFLY-PT polynomials are very complex and, thus, hard to compare, we will calculate the second moment of the polynomials, a strategy to quantify their *spread*, as a means to compare structural differences of the polygonal models for the knots.

The HOMFLY-PT polynomials of a closed Conway and a Kinoshita-Terasaka knot are the same as they are related by mutation [10]:

$$(2*\ell^{-2}+7+6*\ell^{2}+2*\ell^{4})+(-3*\ell^{-2}-11-11*\ell^{2}-3*\ell^{4})*m^{2}+(\ell^{-2}+6+6*\ell^{2}+\ell^{4})*m^{4}+(-1-\ell^{2})*m^{6}$$

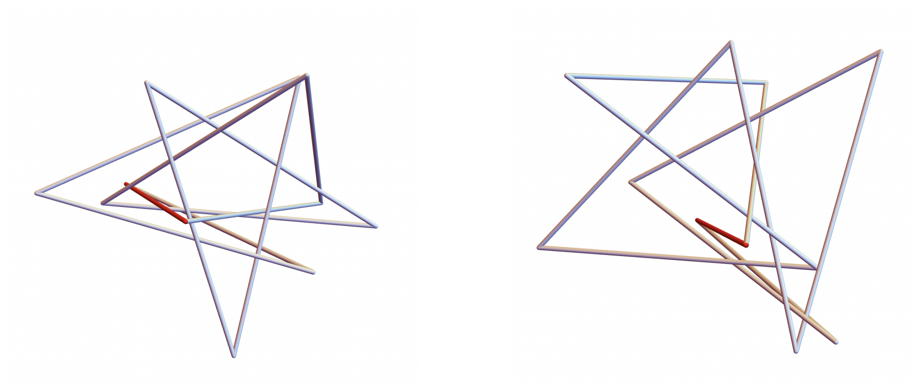

Figure 3: 11 edge equilateral presentations of the closed Conway and the closed Kinoshita-Terasaka knots

2 Spectra, superposition, HOMFLY-PT polynomials, and spread

In this study, we are focused on polygonal repesentations of knots, specifically the presention of the Conway and Kinoshita-Terasaka knots as equilateral 11-edge polygons. Some general facts establish important features of this study. First, there are only a finite number of knot types that can be represented by polygons with a fixed number of edges. Second, every knot is, uniquely up to order, the connected sum of prime (irreducible) knot types [21]. In our case, where we remove an edge from a 10-edge polygon and form a 2-edge closure, every 12-edge polygonal knot is the connected sum of knots from a finite collection of prime knots. Let $\mathscr{K}$ denote the real vector space with this finite set of prime knot types as basis.

One of the important tools to identify prime knot types has been the Alexander polynomial [1], a one variable integer polynomial calculated from a presentation of a configuration. If the Alexander polynomial of two configurations differed by more than a multiplicative unit, the configurations must represent different knot types. However, if the polynomials were equivalent, the relationship of the knots was not established. In the 1980's the Jones polynomial [7] was discovered and was observed to have properties similar to the Alexander polynomial, i.e the "skein relations", connecting the polynomials of three related representations. Shortly thereafter, generalizations of these polynomials, HOMFLY-PT [4, 10] and Kauffman [8], were discovered thereby providing more methods to study and uncover properties of knots. They all enjoy the property that if they differ, the knots differ, and that they are more effective in distinguishing knots. Alas they too have small families of knots that they are unable to distinguish. Principal among such families are the mutant knots which have the same polynomials, a consequence of the skein theory.

The HOMFLY-PT polynomial, [10], $P_L(\ell, m)$ is a finite Laurent two variable

Figure 4: The skein relations defining the HOMFLY-PT polynomial

polynomial satisfying the following relations:

$$P_O(\ell, m) = 1$$

where O denotes the unknot

$$\ell P_{L_+}(\ell, m) + \ell^{-1} P_{L_-}(\ell, m) + m P_{L_0}(\ell, m) = 0$$

where L_+ , L_-, and L_0 are three oriented links that are identical except near a point where they are as in figure 4.
The HOMFLY-PT polynomials of the simplest knots are found in Table 1.

Among the elementary properties of the HOMFLY-PT polynomial is that the polynomial of a mirror reflection, i.e. reversing all crossings, takes ℓ to ℓ^{-1} in the polynomial. Another, is that the polynomial of a connected sum of knots is the product of the polynomials of the constituent knots.

2.1 The Analysis of Open Chains

The presence of knots in open arcs has a long human history but the need for a mathematical basis for the study of knotting is perhaps founded on the search for conclusive evidence of knotting in proteins. A useful strategy to identify knot in open arcs was provided in 2005, the DMS method [13]. Briefly, this method employes the HOMFLY-PT polynomial to identify the knot type of fixed open polygonal arc each of whose termini are connected to a point on the "2-sphere at infinity." Less poetically, parallel rays that originate at each termini are joined at a great distance from the open arc, figure 5. This gives a closed polygon and a knot type for each direction, i.e. each point on the unit 2-sphere, that is well-defined except for a set of measure zero corresponding to directions causing self-intersections of the associated polygon. The determination is a locally constant function to a finite collection of possible knot types. To estimate the probability distribution of knot types one can use a stochastic approach or sample a large collection of uniformly distributed points on the 2-sphere. In this way, one can estimate the proportion of the closures giving any specific knot type.

One can view the DMS method as an example of a tomographic strategy whereby a spatial structure is to be reconstructed using a finite collection of representations. Here, each closure to the sphere at infinity is viewed as the analysis

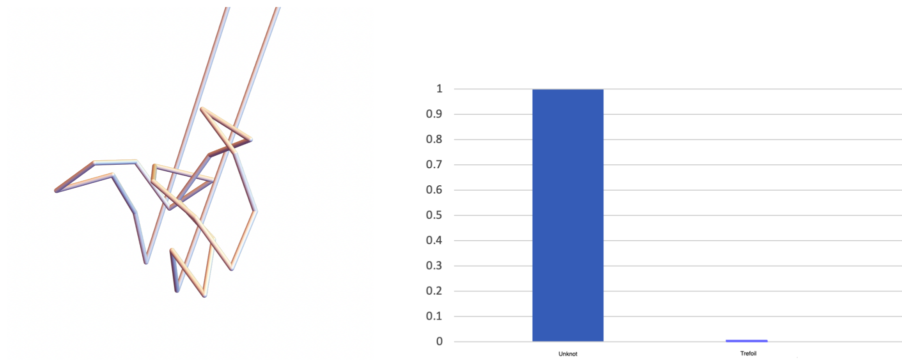

Figure 5: A closure of an equilatural chain, on the left, and a histogram of the spectrum of the knot types of 6400 closures: Unknot 0.9982125, Trefoil 0.001875.

of the orthogonal projection to a plane, the over-crossing closure, [12, 14], between the projected termini composed with the determination of the HOMFLY-PT polynomial the superposition of which gives the state of that projection. Here, the resulting HOMFLY-PT can be described as the representation of the reconstruction determined by the finite collection of projections giving an estimation of the probability distribution on the 2-sphere.

2.2 The Knotting Spectrum

A histogram of the proportion of the knot types observed from the 2-sphere closures gives an estimation of the 2-sphere probability distribution function of knot types: the *knotting spectrum* [13]. A histogram representing the knotting spectrum for a short equilateral chain is shown in figure 5.

The knotting spectrum of a configuration has been employed to detect the presence of a dominant knot type which could be used to describe the topological type of a fixed open chain [15, 19, 22]. Although this knot type changes under spatial isotopy and is, therefore not a “classical topological invariant,” it does provide a useful tool to assess the knottedness of an open chain as a function of its position. For example, in [15], it was observed in a study of 1000 random walks, the assignment of a dominant knot type was possible in 99.6% of cases. However, with this dominant knot-type assignment, many open chains with very different conformations from each other and of possible interest in applications, are assigned to the same knot-type. For example, some significantly complex configurations may be designated as a trivial knot.

2.3 HOMFLY-PT superposition

The *average HOMFLY-PT polynomial* of an open chain is defined as the superposition of the chain’s HOMFLY-PT polynomial spectrum or, equivalently, the integral of the 2-sphere probability distribution of the HOMFLY-PT polynomial given by the function for the configuration over the 2-sphere of closure directions. The spectrum of an open chain can be thought of as a unit vector in the knot space $\mathscr{K}$ whose coordinates are equal to the proportion of the directional 2-sphere whose closures give this knot type. By assigning the HOMFLY-PT to each knot type and taking the sum, one defines a linear transformation from the knot space $\mathscr{K}$ to the ring of real finite Laurent polynomials in ℓ and m. This image is defined to be the average HOMFLY-PT polynomial of the open chain giving this spectrum. In this way we attain the superposition by employing a uniformly distributed set of 6400 points on the 2-sphere, determining the HOMFLY-PT polynomial at each of these points, and taking the weighted sum of the polynomials, thereby giving desired estimation of the average HOMFLY-PT polynomial of the chain. Because the chain in figure 5 is so simple, its average HOMFLY-PT polynomial is

$$0.9981 - 0.00375\ell^2 - 0.00187\ell^4 + 0.00187\ell^2 m^2$$

very close to the polynomial for the unknot, $P_0(\ell, m) = 1$.

2.4 The Spread of Polynomials

Historically, the complexity of a knot has been measured by the number of crossing in a minimal crossing presentation of the knot. Here, however, we propose to employ the HOMFLY-PT to calculate an alternative approach. Therefore we propose a new measure of the complexity of a finite integral Laurent polynomial such as the HOMFLY-PT,

$$P(\ell, m) = \sum_{i=-k, j=-n}^{i=k, j=n} a_{i,j} \ell^i m^j$$

Each point with coordinates (i, j) of the $2k \times 2n$ 2-dimensional integral lattice given the value $|a_{i,j}|$. In analogy with a physical system, we determine the total mass, M, and the ‘”center of mass”, (μ_ℓ, μ_m) of this system:

$$M = \sum_{i=-k, j=-n}^{i=k, j=n} |a_{i,j}|$$

$$(\mu_\ell, \mu_m) = \frac{1}{M} \sum_{i=-k, j=-n}^{i=k, j=n} |a_{i,j}|(i, j)$$

We then define the *spread* of $P(\ell, m)$ in analogy with squared radius of gyration of a physical system:

$$sp(P(\ell, m)) = \frac{1}{M} \sum_{i=-k, j=-n}^{i=k, j=n} |a_{i,j}|((i - \mu_\ell)^2 + (j - \mu_m)^2)$$

The spead of the HOMFLY-PT polynomial of the chain in figure 5 is 1.08431 indicating that it is close to a constant polynomial as suggested by the coefficients.

The spread of the HOMFLY-PT polynomials of the simplest knots and their spreads are given in Table 1.

Knot Type	**HOMFLY-PT polynomial**	**Spread**
0_1	1	0
3_1	$(-2\ell^2 - \ell^4) + \ell^2 m^2$	1.5
4_1	$(-\ell^{-2} - 1 - \ell^2) + m^2$	7.25
5_1	$(3\ell^4 + 2\ell^6) + (-4\ell^4 - \ell^6)m^2 + \ell^4 m^4$	10.517
5_2	$(-\ell^2 + \ell^4 + \ell^6) + (\ell^2 - \ell^4)m^2$	8.26
6_1	$(-\ell^{-2} + \ell^2 + \ell^4) + (1 - \ell^2)m^2$	6.58
6_2	$(2 + 2\ell^2 + \ell^4) + (-1 - 3\ell^2 - \ell^4)m^2 + \ell^2 m^4$	23.29
6_3	$(\ell^{-2} + 3 + \ell^2) + (-\ell^{-2} - 3 - \ell^2)m^2 + m^4$	47.34

Table 1: The HOMFLY-PY polynomials of some simple knots and their spreads.

Having the same HOMFLY-PT polynomials, the spread of the closed Conway & Kinoshita-Terasaka knots is 2058.38.

3 HOMFLY-PT polynomials for comparable open Conway and Kinoshita-Terasaka knots

Consider the open Conway and open Kinoshita-Terasaka knots, figure 6. We have selected these open configurations having the missing edges passing within the interior of the convex hull of the configurations in order to insure a robust spectrum in both cases. If, for example, one selects an edge lying on the boundary of the convex hull, a large proportion of the closures corresponding to directions in the complementary halfspace would instances of the knot type because union of the edge and the closure would support a triangle move proving the equivalence to the knot type. In contrast, with an interior edge, the corresponding triangle would almost certainly intersect some of the complementary edges thereby givng another knot type. The variation in knot types would seem to capture the complexity of the polygonal structure. It seems possible that the variation in knot types, i.e. the spectra, would capture differences in spatial structure of these two open configurations.

One can understand the spectrum of an open knot as a unit vector in the infinite Real vector space whose basis consists of the infinite set of knot types.

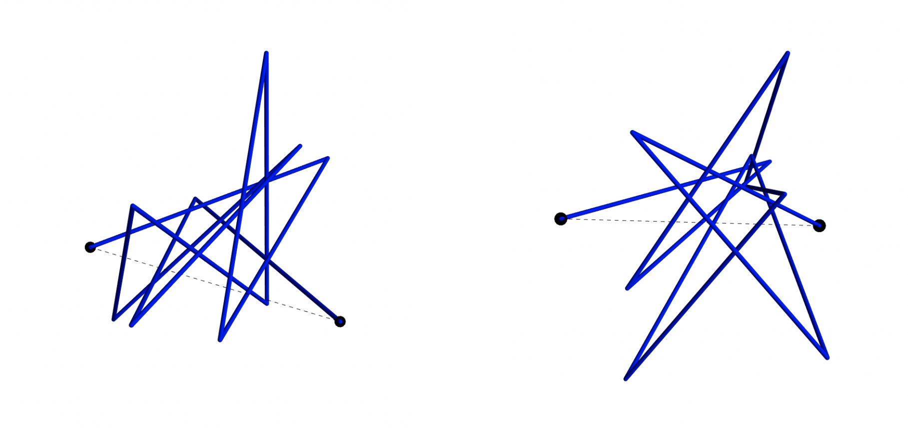

Figure 6: An open 10 edge Conway knot and an open 10 edge Kinoshita-Terasaka knot.

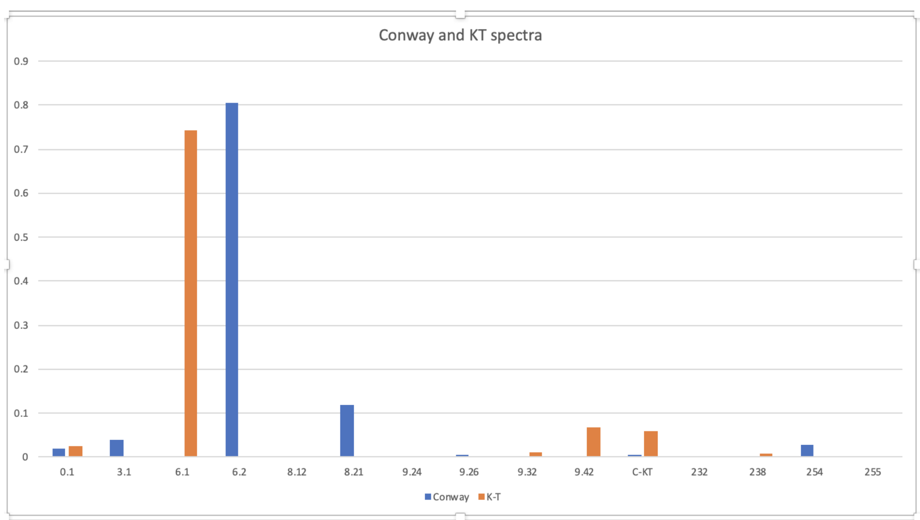

Figure 7: The spectra for the Conway, blue, and K-T, red, open knots, figure 3 corresponding to the data shown in Table 2

HOMFLY-PT Type	Center Open Conway Knot	Center Open Kinoshita-Terasaka Knot
0_1	132	161
3_1	20	18
6_1	0	4702
6_2	5014	22
8_{12}	0	6
8_{21}	755	0
9_{24}	16	0
9_{26}	29	0
9_{30}	0	71
9_{32}	0	510
9_{42}	0	435
C-KT (221)	39	372
$3_1\#3_1$	42	0
$3_1\#-6_2$	144	0
232	17	0
238	0	52
254	189	0
255	3	0

Table 2: The knot types labelled numbers have not yet been identified. Note the substantial difference between the distribution of knot types observed for the 6400 closures for each open configurations shown in figure 6. The associated spectra are shown in figure 7

In the present case, each spectrum is a finite expression in terms of this basis, as shown in Table 2. One defines an inner product in this space in the standard manner (since each vector lives in a finite dimensional subspace) and calculates that the inner product of the spectra for these two open polygonal knot is 0.003574902, showing that the spectra are nearly orthogonal, a fact that is visible in the table 7. Althought this might suggest a significant structural difference between the 10 edge equalateral polygonal models of the Conway and Kinoshita-Terasaka knots, one must take into consideration the choice of missing edges in order to reach such a conclusion. We will do so in a subsequent section.

The HOMFLY-PT superposition takes the spectrum of each polygon to to the associated HOMFLY-PT polynomial of the configuration, figure 6. For the open Conway configuration, this gives

$$P_{Conway}(\ell, m) = (1.5877+1.2071\ell^2+0.4528\ell^4-0.0917\ell^6+0.0066\ell^8)+(-0.7837-2.1120\ell^2-0.4560\ell^4+0.1049\ell^6)m^2+(0.7837\ell^2-0.1144\ell^4)m^4$$

and, for the open K-T configuration, this gives

$$P_{K-T}(\ell,m) = (0.0123\ell^{-4} - 0.8577\ell^{-2} - 0.1737 + 0.589*\ell^{2} + 0.7356\ell^{4}) + (-0.0067\ell^{-4} + 0.0478\ell^{-2} + 1.013 - 0.6686\ell^{2})m^{2} + (0.0034\ell^{-2} - 0.0670)m^{4}$$

The spread of $P_{Conway}(\ell,m)$ is 12.1215 and the spead of $P_{K-T}(\ell,m)$ is 7.3937 indicating that the open Conway knot configuration is likely more complex than the open Kinoshita-Terasaka knot configuration. Another measure of their difference is the spread of $P_{Conway}(\ell,m) - P_{K-T}(\ell,m)$; 22.2807, also demonstrating a substantial difference in the structures of the open configurations.

4 Convergence as gap length goes to zero

As the magnitude of a gap in an edge of a polygonal configuration goes to zero, we know that spectrum of the DMS probability distribution convereges to a constant equal to the knot type of the closed polygonal knot [11]. This implies that the superposition is a continuous function of the polygonal configuration, i.e. the HOMFLY-PY polynomial is a continuous function of the open polygon. As the spread of a polynomial is a continuoius function of the polynomial, the spread of the HOMFLY-PT of an open polygonal configuration is a continuous function of the configuration. In this section, we explore the evolution of the polynomial of the configuration and the associated spread as the length of the gap in an edge changes, figure 8. The data for a sample of gaps is reported in Table 3. We note that it is not until the size of the gap is very small that the HOMPLY-PT polynomial of the arc closely approaches the HOMFLY-PT polynomial of the closed Conway knot, figure 9 as measured by the spread. The HOMFLY-PT polynomials and their corresponding spread are given in Table 3.

Gap: 1.0

$$P_{1.0}(\ell,m) = (-0.109375\ell^{-4} - 0.28375\ell^{-2} + 1.41672 + 1.1325\ell^{2} + 0.43328\ell^{4} - 0.101563\ell^{6} + 0.0066\ell^{8}) + (0.08438\ell^{-4} + 0.3614\ell^{-2} - 0.4620 - 2.0074\ell^{2} - 0.42078\ell^{4} + 0.11469\ell^{6})m^{2} + (-0.13296\ell^{-2} - 0.19156 + 0.707188\ell^{2} - 0.13234\ell^{4})m^{4} + (0.05125 + 0.0164\ell^{2} + 0.00266\ell^{4})m^{6} - 0.00266\ell^{2}m^{6}$$

The spread of $P_{1.0}(\ell,m)$ is 21.294.

Gap: 0.75

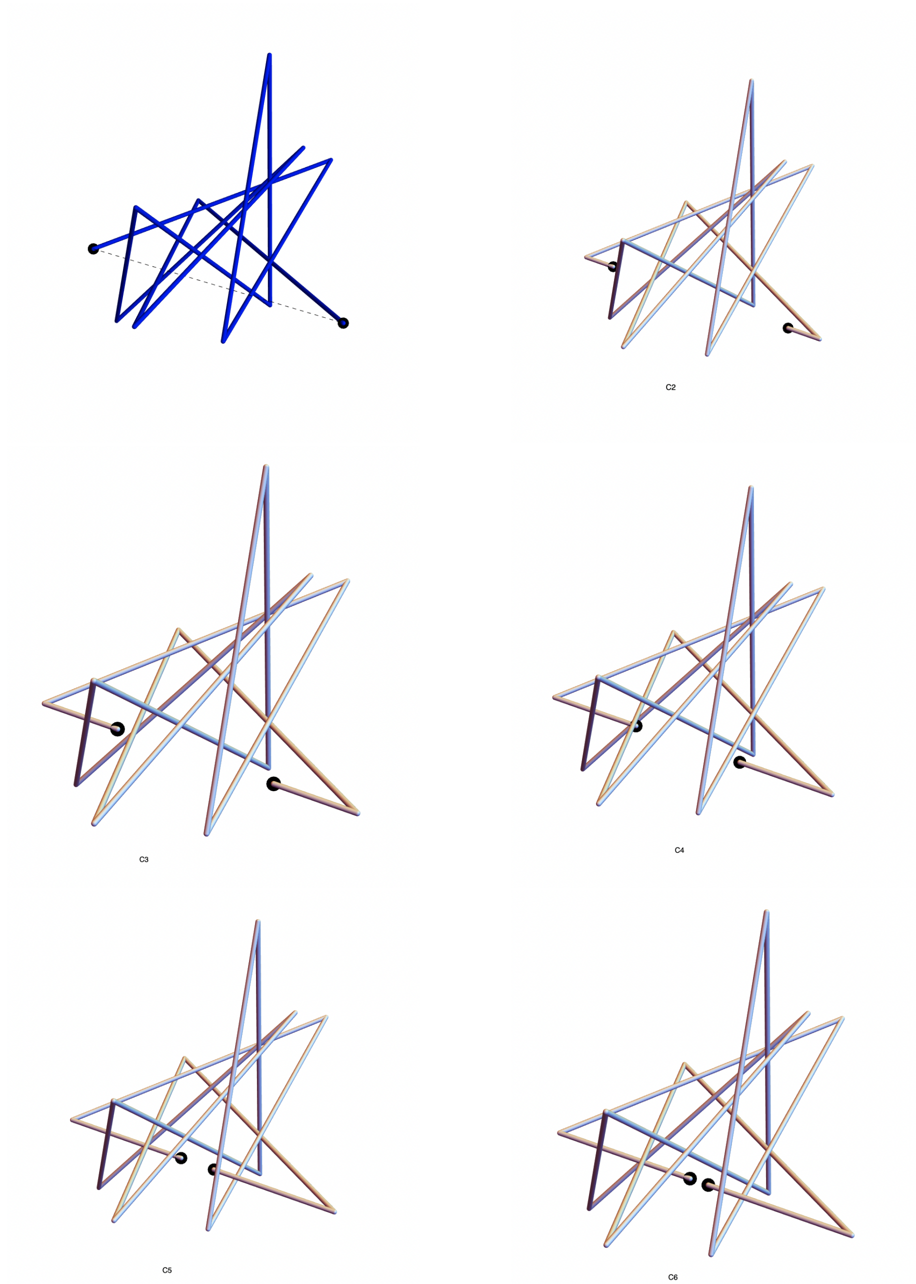

Figure 8: Open equilateral Conway knot with varying gaps:C0=1.00, C2=0.75, C3=0.500, C4=0.375, C5=0.125, C6=0.0625

HOMFLY-PT Type	**1.0**	**0.75**	**0.5**	**0.375**	**0.20**	**0.125**	**0.091**	**0.0625**
0_1	130	250	326	238	52	20	2	3
3_1	20	18	14	0	0	0	0	0
6_1	0	0	0	0	0	0	0	0
6_2	5014	3566	1840	814	6	2	1	1
8_{17}	0	0	0	319	183	58	37	20
8_{21}	755	1838	3075	2972	1278	853	612	417
9_{24}	16	31	48	51	8	0	0	0
9_{26}	29	27	17	5	0	0	0	0
9_{42}	0	5	9	18	0	0	0	0
C-KT (221)	39	74	154	382	2827	3999	4641	5147
$3_1\#3_1$	42	81	69	0	0	0	0	0
$3_1\# -6_2$	144	169	259	295	278	205	159	127
232	17	27	0	106	142	87	57	40
254	0	0	67	136	0	0	0	104
255	190	302	459	535	38	2	0	0
256	4	12	68	137	751	611	460	354
257	0	0	0	386	162	0	0	0
258	0	0	0	0	0	0	0	0
259	0	0	0	0	0	0	0	0
268	0	0	0	0	227	273	213	150
342	0	0	0	41	315	227	181	105
343	0	0	6	12	26	29	222	1
344	0	0	4	89	108	34	15	7

Table 3: Closure data for the open Conway knots with changing gap. The knot types labelled numbers have not yet been identified. The knot types observed for the 6400 closures for each open configuration is shown in figure 8.

$$P_{0.75}(\ell,m) = (-0.156874\ell^{-4} - 0.3970\ell^{-2} + 0.9392 + 0.1675\ell^2 - 0.27375\ell^4 - 0.24922\ell^6 + 0.0127\ell^8) + (0.12562\ell^{-4} + 0.5084\ell^{-2} - 0.15234 - 0.9989\ell^2 + 0.28703\ell^4 + 0.2745\ell^6)m^2 + (-0.1925\ell^{-2} - 0.24594 + 0.47125\ell^2 - 0.2991\ell^4)m^4 + (0.0711 + 0.0203\ell^2 + 0.00422\ell^4)m^6 - 0.00422\ell^2 m^8$$

The spread of $P_{0.75}(\ell,m)$ is 21.294.

Gap: 0.5

$$P_{0.5}(\ell,m) = (0.00125\ell^{-6} - 0.23687\ell^{-4} - 0.5936\ell^{-2} + 0.35766 - 0.9392\ell^2 - 1.1181\ell^4 - -0.45625\ell^6 + 0.0108\ell^8 + 0.0108\ell^8) + (-0.00063\ell^{-6} + 0.187656\ell^{-4} + 0.7448\ell^{-2} + 0.2278 + 0.13016\ell^2 + 1.126\ell^4 + 0.47781\ell^6)m^2 + (0.00125\ell^{-4} - 0.2845\ell^{-2} - 0.32406 + 0.2178\ell^2 - 0.49625\ell^4)m^4 + (-0.0006\ell^{-2} - 0.2845 + 0.02266\ell^2 + 0.0081\ell^4)m^6 -$$

$0.0081\ell^2 m^8$

The spread of $P_{0.5}(\ell, m)$ is 22.308.

Gap: 0.375

$P_{0.375}(\ell, m) = (0.16125\ell^{-6} + 0.05359\ell^{-4} - 0.52421\ell^{-2} + 0.2464 - 1.10812\ell^2 - 1.24156\ell^4 - 0.4648\ell^6) + (-0.0806\ell^{-6} - 0.281719\ell^{-4} + 0.40781\ell^{-2} + 0.1846875 + 0.3775\ell^2 + 1.242969\ell^4 + 0.49828\ell^6)m^2 + (0.18047\ell^{-4} + 0.03109\ell^{-2} - 0.29437 + 0.12281\ell^2 - 0.4989\ell^4)m^4 + (00.11265\ell^{-2} + 0.13797 + 0.00594\ell^2)m^6$

The spread of $P_{0.375}(\ell, m)$ is 23.5165.

Gap: 0.2

$P_{0.125}(\ell, m) = (0.1828\ell^{-6} + 0.24265\ell^{-4} + 0.593125\ell^{-2} + 2.9966 + 1.925\ell^2 + 0.2514\ell^4 - 0.49828\ell^6) + (-0.0914\ell^{-6} - 0.56859\ell^{-4} - 1.4125\ell^{-2} + 0.18468 - 4.4051\ell^2 - 0.70359\ell^4 + 0.24406\ell^6)m^2 + (0.330469\ell^{-4} + 0.8664\ell^{-2} + 2.1000 + 2.5255\ell^2 + 0.208125\ell^4)m^4 + (-0.04919\ell^{-4} - 0.3020\ell^{-2} - 0.1414 - 0.4061\ell^2 + 0.02219\ell^4)m^6 + (0.04922\ell^{-2} - 0.03547 - 0.02219\ell^2)m^8$

The spread of $P_{0.2}(\ell, m)$ is 386.603.

Gap: 0.125

$P_{0.125}(\ell, m) = (0.08156\ell^{-6} + 0.04859\ell^{-4} + 0.9328\ell^{-2} + 4.2432 + 3.2823\ell^2 + 0.8550\ell^4 - 0.16047\ell^6) + (-0.04078\ell^{-6} - 0.233\ell^{-4} - 1.6703\ell^{-2} - 6.3623 - 6.60609\ell^2 - 1.5119\ell^4 + 0.1605\ell^6)m^2 + (0.18796\ell^{-4} + 0.734531\ell^{-2} + 3.1484 + 3.67719\ell^2 + 0.4964\ell^4)m^4 + (-0.03547\ell^{-4} - 0.175469\ell^{-2} - 0.306718 - 0.597656\ell^2 + 0.013594\ell^4)m^6 + (0.03547\ell^{-2} - 0.04266 - 0.01359\ell^2)m^8$

The spread of $P_{0.125}(\ell, m)$ is 709.882.

Gap: 0.091

$P_{0.091}(\ell, m) = (0.06125\ell^{-6} + 0.03453\ell^{-4} + 1.2089\ell^{-2} + 4.9720 + 4.02172\ell^2 + 1.1766\ell^4 - 0.1134\ell^6) + (-0.30624\ell^{-6} - 0.17719\ell^{-4} - 2.017\ell^{-2} - 7.58578 - 7.8006\ell^2 - 1.9325\ell^4 + 0.1134\ell^6)m^2 + (0.1460\ell^{-4} + 0.81374\ell^{-2} + 3.89266 + 4.3128\ell^2 + 0.6425\ell^4)m^4 +$

$(-0.0282\ell^{-4} - 0.13875\ell^{-2} - 0.4809 - 0.7048\ell^2 + 0.0089\ell^4)m^6 + (0.0283\ell^{-2} - 0.03328 - 0.0089\ell^2)m^8$

The spread of $P_{0.091}(\ell, m)$ is 1019.21.

Gap: 0.0625

$$P_{0.0625}(\ell, m) = (0.0350\ell^{-6} + 0.04672\ell^{-4} + 1.5519\ell^{-2} + 5.6666 + 4.6545\ell^2 + 1.4428\ell^4 - 0.7765\ell^6) + (-0.0175\ell^{-6} - 0.1344\ell^{-4} - 2.5284\ell^{-2} - 8.9334 - 8.8961\ell^2 - 2.2595\ell^4 + 0.0777\ell^6)m^2 + (0.08422\ell^{-4} + 0.9791\ell^{-2} + 4.8663 + 4.9369\ell^2 + 0.7539\ell^4)m^4 + (-0.0164\ell^{-4} - 0.0995\ell^{-2} - 0.7914 - 0.8191\ell^2 + 0.0063\ell^4)m^6 + (0.0164\ell^{-2} - 0.0063\ell^2)m^8$$

The spread of $P_{0.0625}(\ell, m)$ is 1396.77.

For comparison, we note that, for our closed Conway knot, one has

$$P_{Conway}(\ell, m) = (2 * \ell^{-2} + 7 + 6 * \ell^2 + 2 * \ell^4) + (-3 * \ell^{-2} - 11 - 11 * \ell^2 - 3 * \ell^4) * m^2 + (\ell^{-2} + 6 + 6 * \ell^2 + \ell^4) * m^4 + (-1 - \ell^2) * m^6$$

The spread of $P_{Conway}(\ell, m)$ is 2058.38.

5 Superposition over all 11 edge gaps

As a new strategy to measure and compare the structural complexity of these 11-edge equilateral Conway and Kinoshita-Terasaka knot models we analyze the HOMFLY-PT superposition of the ensemble of all 11 edge gap configurations for both structures. With 6400 closures for each of the gaps, we have a collection of 70,400 closures for each. As a consequence, the associated spectra,, whose joint distributions give the average HOMFLY-PT polynomial, does not depend on an edge selection and, thereby, provides a robust comparison of these two configuration.

For the open Conway knot, 97 different HOMFLY-PT polynomials are observed. Their superposition is

$$P_{Conway11}(\ell, m) = (-0.0.0011\ell^{-8} + 0.1518\ell^{-6} + 0.3889\ell^{-4} + 0.8112\ell^{-2} + 2.2906 + 0.9147\ell^2 + 0.2025\ell^4 + 0.0017\ell^6 + 0.0058\ell^8 - 0.0012\ell^{10}) + (0.0002\ell^{-8} - 0.0011\ell^{-6} -$$

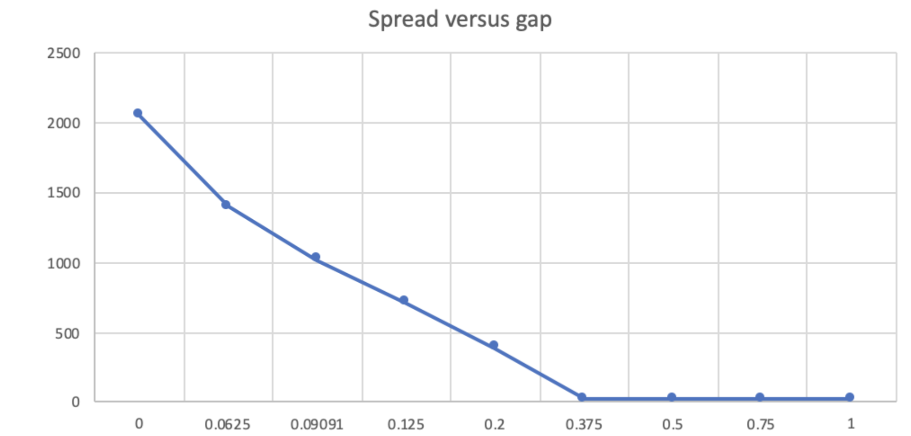

Figure 9: Spread(HOMFLY-PT) versus the gap in a selected interior edge of the Conway polygon, figure 8

$$0.2669\ell^{-4} - 1.0300\ell^{-2} - 2.4790 - 1.9111\ell^{2} - 0.3651\ell^{4} + 0.0779\ell^{6} - 0.0021\ell^{8})m^{2} + (-0.0003\ell^{-6} + 0.0011\ell^{-4} + 0.3913\ell^{-2} + 1.5770 + 1.1355\ell^{2} + 0.0596\ell^{4} + 0.0008\ell^{6} - 0.00001\ell^{8})m^{4} + (0.0012\ell^{-4} + 0.0045\ell^{-2} - 0.2768 - 0.12300\ell^{2} + 0.00001\ell^{4} - 0.0003\ell^{6})m^{6} + (-0.0011\ell^{-2} - 0.0010 - 0.0056\ell^{2} + 0.0003\ell^{4})m^{8}$$

The spread of $P_{Conway11}(\ell, m)$ is 119.089 whereas the spread of the closed Conway and Kinoshita-Terasaka HOMFLY-PT polynomial knot is 2058.38.

For the open Kinoshita-Terasaka knot, 86 different HOMFLY-PT polynomials are observed. Their superposition is

$$P_{KT11}(\ell, m) = (-0.0007386\ell^{-8} + 0.0220454\ell^{-6} - 0.264631\ell^{-4} - 0.339318\ell^{-2} + 1.330753 + 0.139105\ell^{2} - 0.364489\ell^{4} - 0.224929\ell^{6} + 0.0126989\ell^{8} - 0.00001\ell^{10}) + (-0.000369\ell^{-8} - 0.00821\ell^{-6} + 0.02598\ell^{-4} + 0.10460\ell^{-2} - 1.504616 - 1.16983\ell^{2} + 0.39116\ell^{4} + 0.239886\ell^{6} - 0.01332\ell^{8} + 0.000071\ell^{10})m^{2} + (-0.000696\ell^{-6} + 0.015994\ell^{-4} - 0.00656\ell^{-2} + 0.887599 + 0.78575\ell^{2} - 0.16528\ell^{4} + 0.001676\ell^{6} + 0.000227\ell^{8} + 0.000028\ell^{10})m^{4} + (0.000282\ell^{-4} - 0.00656\ell^{-2} - 0.116321 - 0.152287\ell^{2} - 0.013523\ell^{4} + 0.01229\ell^{6} + 0.0000568\ell^{8})m^{6} + (-0.0000426\ell^{-2} - 0.00004 - 0.000355\ell^{2} + 0.000128\ell^{4} - 0.000028\ell^{6})m^{8}$$

The spread of $P_{KT11}(\ell, m)$ is 36.9532 whereas the spread of the Conway and Kinoshita-Terasaka HOMFLY-PT polynomial knot is 2058.38.

The spread of KT11 - Conway11 is 90.4808, providing a measure of the significance of the difference between the two HOMFLY[PT polynomials.

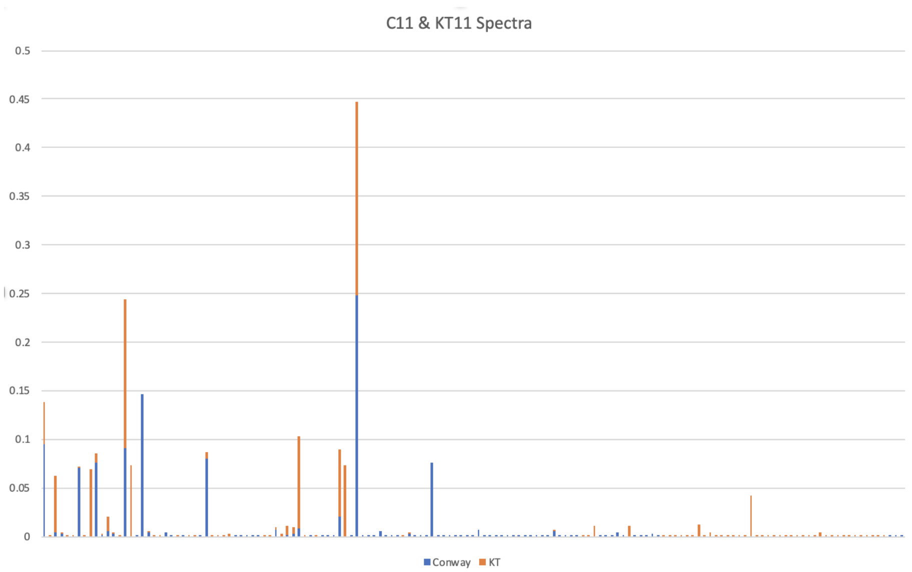

Figure 10: The spectra for the Conway11, blue, and K-T11, red, collection of 11 edge gaps illustrating the distinct charater of the knots.

From this HOMFLY-PT data, we propose that there is an important structural difference between the 11 equilateral edge presentations of the Conway and Kinoshita-Terasaka knots with the Conway conformation being significantly more complex.

5.1 The spectrum of Conway11 versus spectrum of Kinoshita-Terasaka11

A finer comparision of the Conway and Kinoshita-Terasaka 11 equilateral edge polygonal models can be accomplished by comparing the spectra, figure 10, where one observes specific instances of differences in the observed HOMFLY-PT polynomials giving distinct points in the knot space. Their inner product is 0.071 suggest the weak relationship shown in the spectra.

From this HOMFLY-PT spectral data, we again conclude that there is an important structural difference between the 11 equilateral edge presentations of the Conway and Kinoshita-Terasaka knots.

6 Conclusions

The Conway knot and the Kinoshita-Terasaka knots are different since Riley's study of finite group representations of the fundamental groups of knot complements [20], Gabai [5] has proved that they have different genera and, more recently, Morton and Cromwell [16] have used knot polynomials satallites to show they are distinct. Nevertheless, having an elementary reason for their difference is still an attractive goal in as much as they are mutants. To identify a structural feature that might identify some helpful structural feature, we have exploited our ability to highlight structural features of an open arc by applying the DMS method to open arcs based on 11 edge equilateral polygonal models of the two knots. Of course the DMS spectrum depends on the chosen edge, so we consider the entire collection of 11 edge gaps for each knot. Comparison of the spectra is complex so, inspired by [17], we have computed the DMS superposition giving the average HOMFLY-PT polynomial of the open arc. To further simplify the analysis, we defined the spread of a polynomial giving a measure of the complexity of the superposition. Both provide measures of the independence of the superposition and differences in complecity. These provide a new perspective on the difference between the Conway and Kinoshita-Terasaka conformations. Although our analysis is limited to a small number of open portions of the specific polygonal models, they could lead to clues as to features of the two knots that caputure facets that distinguish them.

There are fundamental questions that are worthy of study. First, can one discern geometric features of a configuration represented in the structure of the superposition HOMFLY-PT polynomial of the collection of edge complements? Furthermore, are there facets in common for these HOMFLY-PT polynomials for different equilateral presentations of a given knot type? Answers to such questions might provide a strategy to help determine whether or not there are geometrically distinct equilateral polygonal conformations that are topologically unknotted.

References

[1] J. W. Alexander. Topological invariants of knots and links. *Trans. Amer. Math. Soc.*, 30(2):275–306, 1928.

[2] J. H. Conway. An enumeration of knots and links, and some of their algebraic properties. In *Computational Problems in Abstract Algebra (Proc. Conf. Oxford, 1967)*, pages 329–358. Pergamon, Oxford, 1970.

[3] T. D. Eddy and C Shonkwiler. New stick number bounds from random sampling of confined polygons. *arXiv*, pages 1–35, 2019.

[4] P. Freyd, D. Yetter, J. Hoste, W. B. R. Lickorish, K.C. Millett, and A. Ocneanu. A new polynomial invariant of knots and links. *Bull. Amer. Math. Soc. (N.S.)*, 12(2):239–246, 1985.

[5] D. Gabai. Genera of the arborescent links. *Memoirs of the Amer. Math. Soc.*, 59(339):1 – 98, 1986.

[6] J. Hom. Getting a handle on the conway knot, 2021.

[7] V. Jones. Hecke algebra representations of braid groups and link polynomials. *Ann. of Math.*, 126(2):335–388, 1987.

[8] Louis H. Kauffman. An invariant of regular isotopy. *Trans. Amer. Math. Soc.*, 318(2):417 – 471, 1990.

[9] S. Kinoshita and H. Terasaka. On unions of knots. *Osaka Math. J*, 9:131 – 153, 1959.

[10] W. B. R. Lickorish and K. C. Millett. A polynomial invariant of oriented links. *Topology*, 26(1):107 – 141, 1987.

[11] K. C. Millett. The length scale of 3-space knots, ephemeral knots, and slipknots in random walks. *Prog. of Theo. Physics Sup.*, 191:182–191, 2011.

[12] K. C. Millett. Knots in knots: A study of classical knot diagrams. *J. Knot Theory Ramifications*, 25(9):1641013, 10, 2016.

[13] K. C. Millett, A. Dobay, and A. Stasiak. Linear random knots and their scaling behavior. *Macromolecules*, 38(2):601–606, 2005.

[14] K. C. Millett and A. Rich. More knots in knots: a study of classical knot diagrams. *J. Knot Theory Ramifications*, 26(8):1750046, 18, 2017.

[15] K. C. Millett and B. M. Sheldon. Tying down open knots: A statistical method of identifying open knots with applications to proteins. In *Physical and numerical models in knot theory*, volume 36 of *Ser. Knots Everything*, pages 203–217. World Sci. Publishing, Singapore, 2005.

[16] H. R. Morton and P. R. Cromwell. Distinguishing mutants by knot polynomials. *Journal of Knot Theory and its Ramifications*, 5(2):225 – 238, 1996.

[17] E. Panagiotou and L. Kauffman. Knot polynomials of open and closed curves. *Proc. R. Soc. Lond. Ser. A Math. Phys. Eng. Sci.*, 476:20200124, 2020.

[18] L. Piccirillo. The conway knot is not slice. *Annals of Mathematics*, 191(2):581 – 591, 2020.

[19] E. J. Rawdon, K. C. Millett, J. I. Sulkowska, and A. Stasiak. Knot localization in proteins. *Biochem. Soc. Trans.*, 41(2):538–541, 2013.

[20] R. Riley. Homomorphisms of knot groups on finite groups. *Math. Comput.*, 25:603 – 617, 1971.

[21] H. Schubert. Die eindeutige zerlegbarkeiteines knotten in primknotten. *Akad. Wiss. Heidelberg*, 3(57 - 104), 1949.

[22] J. I. Sułkowska, E. J. Rawdon, K. C. Millett, J. N. Onuchic, and A. Stasiak. Conservation of complex knotting and slipknotting patterns in proteins. *Proc. Natl. Acad. Sci. USA*, 109(26):E1715–E1723, 2012.